PRAMANA
— journal of
physics

Vol. 54, No. 5
May 2000
pp. 751–761

Bubbling and bistability in two parameter discrete systems

G AMBIKA and N V SUJATHA
Department of Physics, Maharajas College, Cochin 682 011, India

MS received 31 May 1999; revised 12 April 2000

Abstract. We present a graphical analysis of the mechanisms underlying the occurrences of bubbling sequences and bistability regions in the bifurcation scenario of a special class of one dimensional two parameter maps. The main result of the analysis is that whether it is bubbling or bistability is decided by the sign of the third derivative at the inflection point of the map function.

Keywords. Bubbling; bistability; bimodal chaos; 2 parameter 1-d maps.

PACS Nos 05.45.+b; 05.40.+j

1. Introduction

The studies related to onset of chaos in one-dimensional discrete systems modeled by nonlinear maps, have been quite intense and exhaustive during the last two decades. Such a system normally supports a sequence of period doublings leading to chaos. It is also possible to take it back to periodicity through a sequence of period halvings by adding perturbations or modulations to the original system [1,2]. This has, most often, been reported as a mechanism for control of chaos. In addition, there are features like tangent bifurcations, intermittency, crises etc, that occur inside the chaotic regime and are not of immediate relevance to the present work. However, if the system is sufficiently nonlinear, there are other interesting phenomena like bubble structures and bistability that have invited comparatively less attention. The simplest cases where these are realized are maps with at least two control parameters, one that controls the nonlinearity and the other which is a constant additive one i.e. maps of the type,

$$X_{n+1} = f(X_n,\, a,\, b) = f_1(X_n,\, a) + b. \tag{1}$$

In these maps, if a is varied for a given b, the usual period doubling route to chaos is observed. But when a is kept beyond the first period doubling point a_1, at a point inside the stability window of 2-cycle and b is varied, the first period doubling is followed by a period halving forming a closed loop-like structure called the primary bubble in the bifurcation diagram. Similarly if a is inside the stability window of 4-cycle, and b is tuned, secondary bubbles appear on the arms of the primary bubble. Thus as we shift the map along the a-axis and drift it along the b-axis, the complete bubbling scenario develops in the different slices of the space $(X,\, a,\, b)$. This accumulates into what is known as bimodal chaos–chaos

restricted or confined to the arms of the primary bubble. This can be viewed as a separate scenario to chaos in such systems.

It has been confirmed that the Feigenbaum indices for this scenario with a as control parameter would be the same as the α and δ of the normal period doubling route to chaos [3]. However, detailed RG analysis by Oppo and Politi [4], involving the parameter b also indicates that if a is kept at a critical value, a_c, where bimodal chaos just disappears, then there is a slowing down in the convergence rate leading to an index which is $(\delta)^{1/2}$. This has been experimentally verified in a CO_2 laser system with modulated losses [5]. The bubbling scenario is seen in the bifurcation diagrams of many nonlinear systems like coupled driven oscillators [6,7], oscillatory chemical reactions, diode circuits, lasers [8,9], insect populations [10], cardiac cell simulations [11], coupled or modulated maps [12,13], quasi-periodically forced systems [14], DPCM transmission system [15] and traffic flow systems [16] etc. The very fact that this phenomenon appears in such a wide variety of systems makes it highly relevant to investigate and expose the common factor(s) in them i.e., the underlying basic features that make them support bubbles in their bifurcation scenario. The above mentioned continuous systems require maps with at least two parameters of type (1) to model them, the second additive parameter being the coupling strength, secondary forcing amplitude etc. We note that in all the above referred papers no specific mention is made regarding the mechanism of formation of bubbles, probably because the authors were addressing other aspects of the problem. However, there have been a number of isolated attempts to analyse the criteria for bubble formation in a few typical systems. According to Bier and Bountis [3], the two criteria are: the map must possess some symmetry and the first period doubling should occur facing the symmetry line. Later Stone [17] made these a little more explicit by stating that the map should have an extending tail (with a consequent inflection point) and the inflection point should occur to the right of the critical point of the map. It is clear that this applies only to maps with one critical point. The relation of the extending tail to bubbling is briefly discussed in [18] also.

Bistability is an equally interesting and common feature associated with many nonlinear systems like a ring laser [19] and a variety of electronic circuits [20]. A recent renewal of interest in such systems arises from the fact that they form ideal candidates for studies related to stochastic resonance phenomena [21]. To the best of our knowledge, attempts to study any type of conditions for the occurrence of bistability are so far not seen reported in the literature.

Our motivation in the present work is to generalize the criteria reported earlier for bubbling and put them together with more clarity and simplicity. As a by product, we succeed in stating the conditions for bistability also along similar lines in systems of type (1). We provide a detailed graphical analysis, which leads to a simple and comprehensible explanation for the same in the context of the 1-cycle fixed points of such maps.

The paper is organized as follows. In § 2, the criteria for bistability and bubbling are stated followed by a brief explanation. The graphical analysis taking two simple cubic maps as examples is included in § 3. The analysis and the criteria apply as such to a wide variety of maps belonging to the same class. The relevant results of the study in 15 different maps are condensed into a table in the concluding § 4.

2. The dynamics of bubbling and bistability

For the special class of maps given in (1), the occurence of bubbling/bistability can be traced to the following basic properties of the map function $f(X, a, b)$. *The non-linearity in $f(X, a, b)$ must be more than quadratic.* This implies that, $f'(X, a, b)$ (the prime indicating derivative with respect to X), is non-monotonic in X and there exists at least one inflection point X_i, i.e.,

$$f''(X, a, b)|_{X=X_i} = 0. \tag{2}$$

Then we differentiate the following two cases:

(i) One set of maps belonging to the above class are such that the inflection point X_i corresponds to a minimum of the derivative function, i.e., at $X = X_i$,

$$f'''(X, a, b) > 0. \tag{3}$$

For such maps there exists a value of a viz. a_1, such that

$$f'(X, a_1, b)|_{X=X_i} = -1. \tag{4}$$

By fixing a near a_1, such that $f'(X, a, b)|_{X=X_i} < -1$ and tuning b, the system can be taken through a bubble structure in the bifurcation scenario.

(ii) For the other set of maps, the inflection point X_i, is a maximum of the derivative function, such that

$$f'''(X, a, b)|_{X=X_i} < 0. \tag{5}$$

Then there exists a value of $a = a_1$, where

$$f'(X, a_1, b)|_{X=X_i} = +1. \tag{6}$$

By adjusting a near a_1, such that $f'(X, a, b)|_{X=X_i} > +1$, a bistability region can be observed in the system as the parameter b is varied.

The maps under case (i) are such that for a fixed point X^*_-, which is to the left of X_i, but in the immediate neighbourhood of X_i, $\left|f'(X^*_-, a, b)\right| < 1$, and hence will be stable. Similarly, there is another fixed point X^*_+ to the right and near to X_i such that $\left|f'(X^*_+, a, b)\right| < 1$ is also stable. Now, the second parameter b is simple additive for the class of maps under consideration and hence f' is independent of b. By adjusting b, the fixed point can be shifted such that $f'(X^*_-, a, b)$ becomes equal to -1, the period doubling point of the map. Then X^*_- will give rise to a 2-cycle with elements X^*_1 and X^*_2. Since these are in the neighbourhood of X_i, $f'(X^*_1)$ and $f'(X^*_2)$ will be negative so that the product $f'(X^*_1)f'(X^*_2)$ is positive. With further increase of b, period merging takes place for the 2-cycle, with X^*_1 and X^*_2 collapsing into X^*_+, which is just stable at the point where $f'(X^*_+) = -1$. Thus in the parameter window (b_1, b_2), a bubble structure is formed.

The situation is exactly reversed for case (ii). Here in the neighbourhood of X_i, a fixed point X^*_-, to the left of X_i, will be stable since $|f'(X_i, a, b)| < 1$. Similarly X^*_+ on the right of X_i also will be stable. By adjusting the second parameter b, these will be shifted to their respective tangent bifurcation points, i.e., b_1 where X^*_+ is born and b_2 where X^*_- disappears. Then a bistability window is seen in the interval (b_1, b_2).

3. Graphical analysis

The mechanism of occurrence of bubbling and bistability explained above for maps satisfying the conditions in case (i) and case (ii) respectively can be made more transparent through a detailed graphical analysis. For this we plot the curve C1= $f'(X)$, the 1-cycle fixed point curve C2 = $f(X) - X$ and the 2-cycle curve C3= $f(f(X)) - X$ simultaneously as functions of X, for chosen values of a and b. The zeroes of C2 give the 1-cycle fixed point X^* while those of C3 give the elements of the 2-cycle. Their stability can be checked from the same graph, since the value of the derivative at the fixed points can be read off. We fix the value of a such that $|f'(X_i, a, b)| > 1$. By plotting the above three curves for different values of b, bistability regions or bubbling sequences can be traced for any given map function of type (1).

For further discussion, we consider two specific forms of maps of the cubic type, which are simple but typical examples for cases (i) and (ii). They are

$$\text{M1} : X_{n+1} = b - aX_n + X_n^3, \tag{7}$$

$$\text{M2} : X_{n+1} = b + aX_n - X_n^3. \tag{8}$$

For M1, there are two critical points, $X_{c1} = -\sqrt{a/3}$, which is a maximum and $X_{c2} = \sqrt{a/3}$, which is a minimum. The inflection point occurs in between X_{c1} and X_{c2}, i.e, at $X_i = 0$ where $f''' = 6$. Hence it belongs to case (i) and the value of a_1 as defined by (4) in this case is 1. In figure 1, the three curves mentioned above are plotted for this map at $a = 1.3$. We start from a value of $b = -1.34$, figure 1a, where the fixed point X^*_- is just born via tangent bifurcation since $f'(X^*_-)$ here is $+1$, and the curves C2 and C3 just touches the zero line on the left of X_i at X^*_-. Though C2 has a zero on the right, the slope there is larger than 1 and hence it is unstable, for this value of b. Since b is only additive, increase in the value of b, shifts C2 upwards, resulting in a slow drift of X^*_- from left to right. Thus as b is increased to -0.7 (figure 1b), $f'(X^*_-) = -1$ and X^*_- bifurcates into X^*_1 and X^*_2. At $b = -0.3$ (figure 1c), the 2-cycle is stable with $f'(X^*_1)$ and $f'(X^*_2)$, both negative and their product is positive but less than 1. Note that the curve C3 has developed a maximum and a minimum on both sides of X^*_-, which is now unstable, cutting the zero line again at $X^*_1 < X^*_-$ and $X^*_2 > X^*_-$. As b is further increased, they move apart. Since the value of a chosen is within the stability window of 2-cycle no further period doubling takes place. As X^*_- crosses X_i, X^*_1 and X^*_2 move towards each other and merge together at $b = 0.7$ (figure 1d) and coincide with the fixed point X^*_+. Further, X^*_+ disappears by a reverse tangent bifurcation at $b = 1.34$, when $f'(X^*_+)$ becomes equal to $+1$. Thus the above events lead to the formation of a primary bubble in the window $(-0.7, 0.7)$.

By keeping a at a value beyond the second period doubling point a_2 of the map, the merging tendency starts only after the second period doubling and hence secondary bubbles are seen on the arms of the primary bubble. This can be continued until at $a >= a_\infty$, the system is taken to chaos. These sequence of behaviour are displayed in the bifurcation diagrams (figure 2a–c) obtained numerically by iterating the map M1, 5000 times and plotting the asymptotic values. Figure 2d shows the numerically calculated slopes of the 2-cycle elements X^*_1 and X^*_2 separately and their product $f'(X^*_1)f'(X^*_2)$ within the primary bubble as a function of b. It is easy to see that this is in agreement with the graphical analysis shown in figure 1.

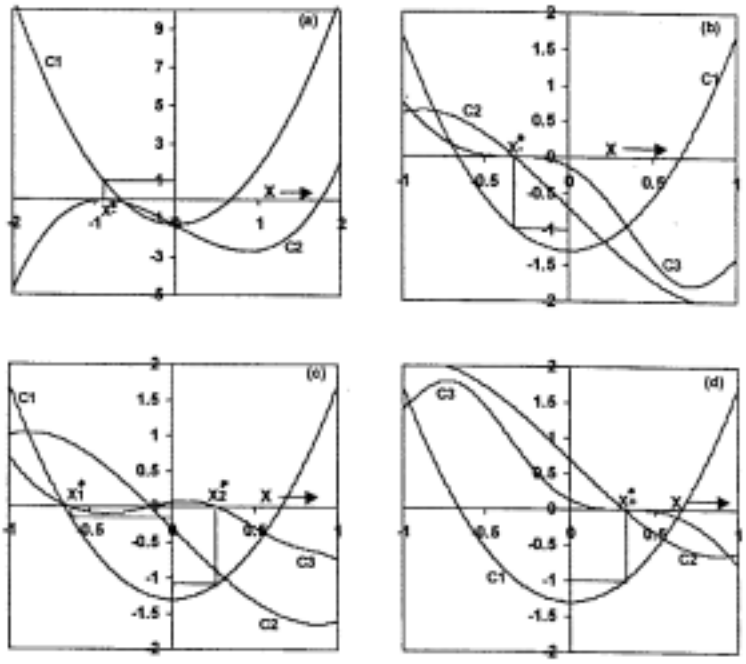

Figure 1. The derivative curve C1, the 1-cycle solution curve C2 and the 2-cycle solution curve C3 plotted with the value of a at 1.3 for the map M1. In **(a)** $b = -1.34$ shows the point where the 1-cycle X^*_- is just born, with $f'(X^*_-) = +1$. **(b)** With $b = b_1 = -0.7$, $f'(X^*_-) = -1$ hence the X^*_- becomes unstable and the 2-cycle is just born. **(c)** $b = -0.3$, shows the elements of the stable 2-cycle with X^*_1 to the left and X^*_2 to the right of the X^*_-, which is unstable now and **(d)** $b = b_2 = +0.7$, the 1-cycle fixed point X^*_+ becomes stable after the merging of X^*_1 and X^*_2.

The stability regions of the different types of dynamical behaviour possible for M1 are marked out in parameter space plot in the (a, b) plane (figure 3). The cone like region on the left is the stability zone of the 1-cycle fixed point (periodicity, $p = 1$) and it is separated from the escape region by the tangent bifurcation line on both sides. The parabola like curve inside it marks out the 2-cycle ($p = 2$) region, while the smaller parabolas indicate curves along which 4-cycles ($p = 4$) and other higher periodic cycles becomes stable until chaos is reached. The line parallel to the b-axis at a value of $a > a_1$, along which primary bubble is formed, is shown by the dotted line. It is clear that along this line, the system is taken from escape $\rightarrow$ 1-cycle $\rightarrow$ 2-cycle $\rightarrow$ 1-cycle $\rightarrow$ escape. Similarly secondary bubbles are formed along a line drawn at $a > a_2$ etc.

Now the above analysis is repeated for map M2, which satisfies the conditions in case (ii) (figure 4). Here, of the two critical points of the map, $X_{c1} = -\sqrt{a/3}$ is the minimum and $X_{c2} = \sqrt{a/3}$ is the maximum with a positive slope at the point of inflection X_i. a_1 in this case is also 1. Hence in figure 4, a is chosen to be 1.4. Figure 4b shows the situation for $b = -0.35$, with $f'(X^*_-) = -1$ where the 1-cycle fixed point X^*_- period doubles into a 2-cycle. For lower values of b, we expect the full period doubling scenario

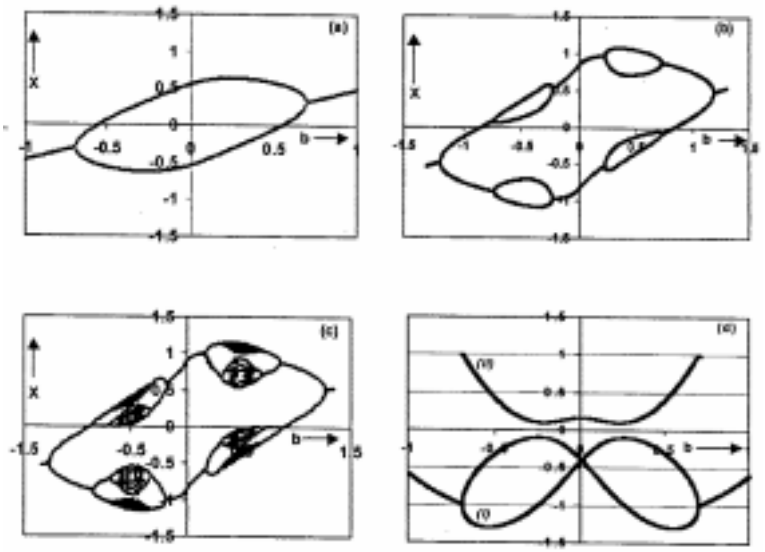

Figure 2. Bifurcation diagrams showing the bubbling sequences for the map M1 with b as the control parameter. **(a)** $a = 1.3$ showing the formation of the primary bubble, **(b)** secondary bubbles at $a = 1.7$, **(c)** bimodal chaos at $a = 1.76$ and **(d)** the derivatives for the 2-cycle elements with $a = 1.3$ calculated numerically and plotted separately as series (I) and their product viz. $f'(X_1^*)f'(X_2^*)$, as series (II).

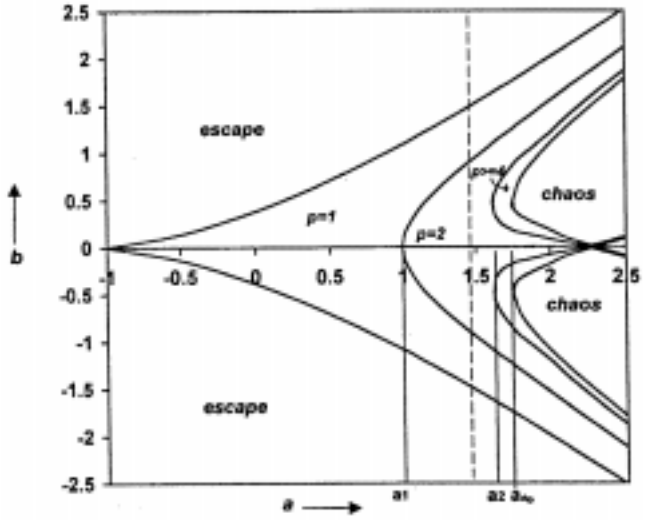

Figure 3. Parameter space plot in $(a,\ b)$ plane for map M1 defined in (7). The minimum a value for having period doubling defined by the eq. (4), viz. a_1, the second period doubling point a_2 and the accumulation point a_∞ are explicitly marked.

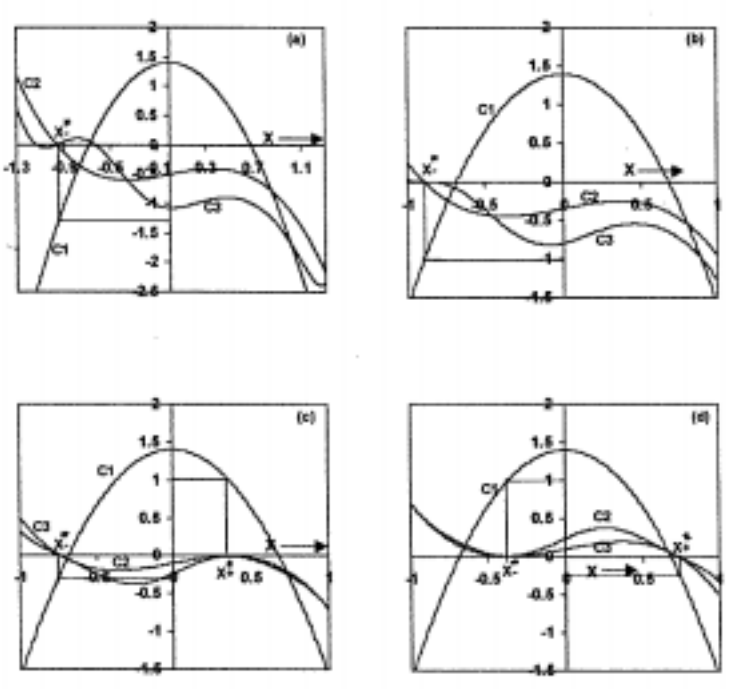

Figure 4. Here the curves C1, C2 and C3 for the map M2 in (8) with $a = 1.4$ is plotted. **(a)** At $b = -0.5$, it is clear from the figure that the 1-cycle solution is unstable and the 2-cycle is stable. **(b)** $b = -0.35$ gives the first period doubling point i.e., here $f'(X_-^*) = -1$. **(c)** At $b = b_1 = -0.1$, $f'(X_+^*) = +1$, i.e., the creation of a new fixed point X_+^* by tangent bifurcation. Note that still X_-^* is stable and **(d)** $b = b_2 = 0.1$, $f'(X_-^*)$ is $+1$. Hence the existing fixed point X_-^* disappears. Thus $(b_1,\ b_2)$ gives the bistability window.

since f' is monotonic beyond this point (figure 4a). However, as b is increased to -0.1, $f'(X_+^*) = +1$, and the other 1-cycle, X_+^* to the right of X_i is born by tangent bifurcation. Note that at this point X_-^* is still stable with $\left|f'(X_-^*)\right| < 1$. This continues until $b = +0.1$, where $f'(X_-^*) = +1$ and hence X_-^* disappears. The birth of X_+^* is concurrent with the maximum of C2 touching the zero line $(b = b_1)$ while the disappearance of X_-^* occurs as the minimum of C2 touches the zero line $(b = b_2)$. As b is increased and C2 is moving up it is clear that the former will take place for a lower b value than the latter, as the maximum of C2 occurs at $X > X_i$ and minimum at $X < X_i$ (slope being positive at X_i). Hence $b_1 < b_2$, or there is a window $(b_1,\ b_2)$, where bistability exists, which in our graph is $(-0.1,\ 0.1)$ for $a = 1.4$. X_+^* is stable beyond this point also and its period doubles as b is increased to $b = +0.35$, where $f'(X_+^*) = -1$. The full Feigenbaum scenario then develops for higher values of b.

By keeping a at higher values and tuning b, the bistability can be taken to 2-cycle, 4-cycle and even chaotic regions. These are shown separately in the bifurcation diagrams plotted numerically for M2 (figure 5). Figure 6 is the parameter space plot in the $(a,\ b)$ plane. The quadrilateral like region marked as (I) beyond $a > a_1$ is the bistable

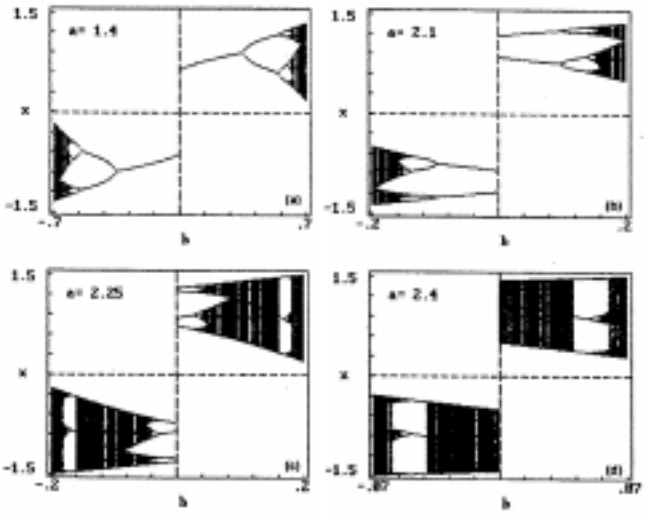

Figure 5. The bifurcation diagrams for the map M2, showing the bistability in the central region. **(a)** $a = 1.4$, shows the 1-cycle bistability and period doubling scenario to both sides, **(b)** $a = 2.1$, shows the 2-cycle bistability, **(c)** the 4-cycle bistability at $a = 2.25$ and **(d)** $a = 2.4$, the bistability can be seen in chaotic regions.

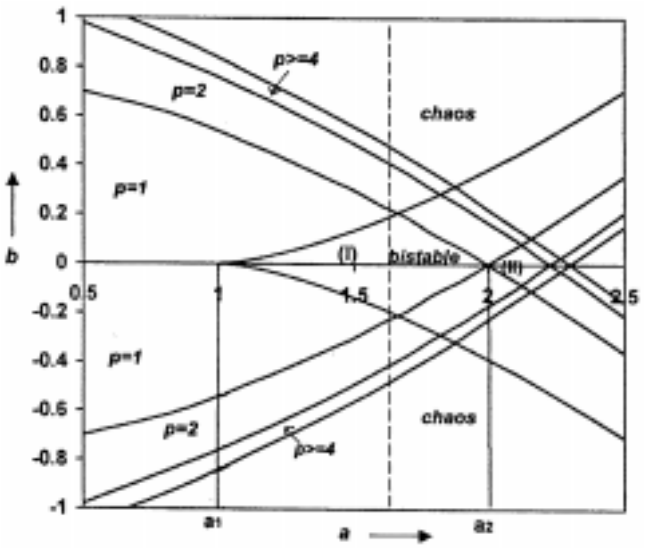

Figure 6. Parameter space plot in (a, b) plane for map M2. The minimum a value for bistability viz. a_1, and the higher order bistability points a_2, etc. are marked. The quadrilateral marked as (I) gives the bistable region for 1-cycle and (II) that for 2-cycle etc.

region for 1-cycle, while quadrilateral (II) is that for 2-cycle etc. The area marked with $p = 1$, is the stability region of 1-cycle while $p = 2$, that for 2-cycle etc. When the system is taken along the dotted line beyond a_1, bistability is seen in the central region, followed by period doubling bifurcations to both sides, until chaos is reached.

4. Conclusion

Although the above discussion is confined to two simple cubic maps, the analysis is repeated for a large number of maps of type (1) chosen from a wide variety of situations covering different functional forms like exponential, trigonometric and polynomial maps. The results are condensed in table 1. We find that the qualitative behaviour in all cases remain the same and depends only on the criteria (2)–(6). Hence the pattern of scenario detailed in this paper can be taken to be atypical as far as maps of the form (1) are concerned.

Table 1. The characteristics of 2 parameter 1-d maps that exhibit bubbling/bistability related to their 1-cycle fixed points.

$f(X)$	X^* at $b = 0$	X_c	X_i	$f'''(X_i)$	Bubble	Bistable
$b + X^3 - aX$	$0, \pm\sqrt{a+1}$	$\pm\sqrt{a/3}$	0	$+6$	Yes	No
$b - X^3 + aX$	$0, \pm\sqrt{a-1}$	$\pm\sqrt{a/3}$	0	-6	No	Yes
$b + aX/(1+X^2)$	$0, \pm\sqrt{a-1}$	± 1	$\pm\sqrt{3}$	$+3a/16$	Yes	No
$b + 5aX/(1+X)^2$	$0, \pm\sqrt{5a-1}$	$1(a=4)$	2	$+0.49$	Yes	No
$4a(X^5 - 5X^3/4 +$	$0, \pm 5, \pm 1$	± 0.35	0	$-30a$	No	Yes
$5X/16) + b$	$(a = 4)$	± 0.8	0.6124	$+60a$	Yes	No
$4aX(1-X)$	0, 3/4	0.15,	0.2959	$+78.3a$	Yes	No
$(1-2X)^2 + b$	$(5 \pm \sqrt{5})/8$ $(a = 4)$	0.5, 0.9	0.7041	$-78.3a$	No	Yes
$b + aX^2 \sin \pi x$	0	0	0.485	-8.5	No	Yes
		± 0.73	1.275	$+23$	Yes	No
$b + \exp(-aX^2)$	0.487 $(a = 3)$	0 ± 1.5	$\pm\sqrt{1/2a}$	$+3.43a^2$	Yes	No
$X \exp(a(1-X)) + b$	0, 1	$1/a$	$+2/a$	$+a^2 e^{(a-2)}$	Yes	No
$X \exp(a(1+X)) - b$	$0, -1$	$-1/a$	$-2/a$	$-a^2 e^{(a-2)}$	No	Yes
$X \exp(a(1+X)) + b, a > 2$	$0, -1$	$-1/a$	$-2/a$	$+a^2 e^{(a-2)}$	Yes	No
$4a(X^3 - 3X^2/2 +$	0, 1/2,1	3/4	1/2	$+24a$	Yes	No
$9X/16) + b$	$(a = 4)$	1/4				
$4aX(1 - 2\sqrt{x} +$	0, 9/16	1/4	9/16	$+7.11a$	Yes	No
$x) + b$	$(a = 4)$	1				
$-a \cos(n(1-x)))$	0.2675	$-8.9,$	-6.4	-0.65	No	Yes
$b + a, n = 2/\pi,$	$(a = 2.5)$	$-3.9, 1,$	-1.45	$+0.6$	Yes	No
$a(2, 5), b(-9, 11)$		5.9,	3.46	-0.6	No	Yes
		10.9	8.4	$+0.65$	Yes	No
$b + \sin(ax)$	0,	$\pm\pi/2a$	0	$-a^3$	No	Yes
	$\pm\sqrt{6(a - 1/a^3)}$		π/a	$+a^3$	Yes	No
			$2\pi/a$	$-a^3$	No	Yes

The criteria for bistability reported here are certainly novel while those for bubbling are more general in nature compared to earlier studies. They can be used as a test to identify maps in which bistability or bubbling is possible and also to isolate the regions in the parameter space (a, b) where they occur. Our main result is that whether it is bistability or bubbling is decided by the sign of the third derivative of the map function at the inflection point. If $f'''(X_i)$ is positive, because of the concave nature of the derivative, tangent bifurcation will precede period doubling as b is increased. Hence bubbling structure is possible. Similarly when $f'''(X_i)$ is negative, curve of f' is convex and hence period doubling precedes tangent bifurcation, leading to bistability. In case $f'''(X_i) = 0$, higher derivatives must be considered for deciding the behaviour. So also when considering bubbling or bistability in higher order cycles the corresponding iterate of the map function must be checked for the inflection point and the sign of the third derivative at that point.

Bubbling can be looked upon as an extreme case of incomplete period doublings and the latter has been often associated with positive Schwarzian derivative [22]. But for the system under study, it is easy to check that this is always negative (independent of the form of the map function), because of properties (2), (3) and (5). In fact, a few such maps have been reported earlier [23] though in a totally different context.

The bubbling scenario in maps of the type M1, leads to bimodal chaos that is restricted to the arms of the primary bubble. Such confined chaos or even low periodic behavior prior to that, makes them better models in population dynamics of ecosystems than the usual logistic type maps [24]. Attempts to extend the criteria to continuous and higher dimensional systems are under way and will be reported elsewhere.

Acknowledgements

SNV thanks the UGC, New Delhi for financial assistance through a junior research fellowship and GA acknowledges the warm hospitality and computer facility at IUCAA, Pune.

References

[1] S Parthasarathy and S Sinha, *Phys. Rev.* **E51**, 6239 (1995)
[2] P R Krishnan Nair, V M Nandakumaran and G Ambika, *Pramana – J. Phys.* **43**, 421 (1994)
[3] M Bier and T Bountis, *Phys. Lett.* **A104**, 239 (1984)
[4] G L Oppo and A Politi, *Phys. Rev.* **A30**, 435 (1984)
[5] C Lepers, J Legrand and P Glorieux, *Phys. Rev.* **A43**, 2573 (1991)
[6] T Hogg and B A Huberman, *Phys. Rev.* **A29**, 275 (1984)
[7] J Kozlowski, U Parlitz and W Lauterborn, *Phys. Rev.* **E51**, 1861 (1995)
[8] C S Wang, Y H Kao, J C Huang and Y S Gou, *Phys. Rev.* **A45**, 3471 (1992)
[9] K Coffman, W D McCormick and H L Swinney, *Phys. Rev. Lett.* **56**, 999 (1986)
[10] T S Bellows, *J. Anim. Ecol.* **50**, 139 (1981)
[11] M R Guevara, L Glass and A Shrier, *Science* **214**, 1350 (1981)
[12] P R Krishnan Nair, V M Nandakumaran and G Ambika, *Computational aspects in nonlinear dynamics and chaos* edited by G Ambika and V M Nandakumaran (Wiley Eastern Publ. Ltd., New Delhi, 1994) p. 144
[13] P P Saratchandran, V M Nandakumaran and G Ambika, *Pramana – J. Phys.* **47**, 339 (1996)
[14] Z Qu, G Hu, G Yang and G Qiu, *Phys. Rev. Lett.* **74**, 1736 (1995)

[15] C Uhl and D Fournier-Prunaret, *Int. J. Bif. Chaos* **5**, 1033 (1995)
[16] X Zhang and D F Jarett, *Chaos* **8**, 503 (1998)
[17] L Stone, *Nature* (*London*) **365**, 617(1993)
[18] S Sinha and P Das, *Pramana – J. Phys.* **48**, 87 (1997)
[19] R Roy and L Mahdel, *Opt. Commun.* **34**, 133 (1980)
[20] L O Chua and K A Stromsmoe, *Int. J. Engg. Sci.* **9**, 435 (1971)
[21] G Nicolis, C Nicolis and D McKerman, *J. Stat. Phys.* **70**, 125 (1993)
[22] D Singer, *Int. J. Appl. Math.* **35**, 260 (1978)
[23] H E Nusse and J A Yorke, *Phys. Rev. Lett.* **27**, 328 (1988)
[24] S Sinha and S Parthasarathy, *Proc. Natl. Acad. Sci. USA* **93**, 1504 (1996)